

Reproducible Manufacturing of Dye-Sensitized Solar Cells on a Semi-automated Baseline

M. Späth*[†], P. M. Sommeling, J. A. M. van Roosmalen, H. J. P. Smit, N. P. G. van der Burg, D. R. Mahieu, N. J. Bakker and J. M. Kroon

Energy Research Centre of the Netherlands (ECN), Solar Energy, PO Box 1, 1755 ZG Petten, The Netherlands

A fully operational baseline consisting of dedicated equipment to process nanocrystalline dye-sensitized solar cell devices has been installed at ECN. This baseline focuses on the production of glass/glass devices with dimensions up to $10 \times 10 \text{ cm}^2$. Present power conversion efficiencies of 6% obtained for cell areas of 2.5 cm^2 are successfully translated to 100 cm^2 devices with an active area of 68 cm^2 by application of identical cell components. The power conversion efficiency with respect to total area was 4%. Processing of a large number of devices in the baseline shows good results in terms of process reliability and yield. The overall yield for a series of 27 devices ($10 \times 10 \text{ cm}^2$) was 96%, while 84% (22 of the remaining 26 devices) generated a cell efficiency within 7% deviation from the average value (4.3%). The reproducibility of the titanium dioxide (TiO_2) colloid synthesis has been investigated. The deviation from the average efficiency (4.9%) of three batches of colloid was at most 3.2%. These results prove that complete device manufacturing of nc-DSC by a baseline process, starting with colloid synthesis is reproducible for surfaces up to $10 \times 10 \text{ cm}^2$. Copyright © 2003 John Wiley & Sons, Ltd.

1 INTRODUCTION

Solar energy has the potential to fulfill an important part of the sustainable energy demand of future generations. With respect to the present status of PV technologies, improvements in three areas have to be made: costs, applicability and sustainability. Semiconductor-grade silicon wafers are still relatively expensive, so great efforts have been put into the development of potentially cheaper thin-film solar cells. Such films may be purely inorganic, such as amorphous silicon, cadmium telluride, copper–indium–diselenide or contain organic materials as an essential part of the device.

An example of the latter is the nanocrystalline dye-sensitized solar cell (nc-DSC) which has attracted a lot of interest since the breakthrough report of O'Regan and Grätzel.¹ This concept is considered as a promising future technology, owing to its inherent cost reduction potential, which is based on the use of inexpensive components, its relatively simple production technology and its wide applicability. This has already resulted in several working prototypes for low-power and high-power applications.

* Correspondence to: M. Späth, Energy Research Centre of the Netherlands (ECN), Solar Energy, PO Box 1, 1755 ZG Petten, The Netherlands.
[†]E-mail: spath@ecn.nl

Contract/grant sponsors: Novem, ECN-ENGINE; contract/grant number: 146-120-021-1.

The working principle of the nc-DSC differs considerably from that of conventional inorganic solar cells. In contrast to semiconductor $p-n$ junctions, the processes of light absorption and charge transport in a nc-DSC occur in different materials, which avoids the premature recombination of electrons and holes. Owing to the separation of functions, no ultrapure materials are required for a good performance. Incident light is absorbed by a dye that is coated as a monolayer on a transparent nanoporous semiconductor (i.e., TiO_2). The porosity induces an enlargement of the effective surface area up to a factor of about 1000 for layer thickness of $10\ \mu\text{m}$. More dye molecules can be adsorbed onto the surface, which guarantees sufficient light absorption. Photoexcitation of the dye leads to injection of electrons in the conduction band of the oxide. The oxidized dye accepts electrons from iodide ions present in an organic solvent-containing electrolyte. The resulting triiodide is reduced back to iodide ions at a platinum-coated counter-electrode, and an external load completes the electrical circuit. Maximum power conversion efficiencies up to 11% have been achieved for single cells on small active areas² ($<1\ \text{cm}^2$) and up to 8.2%^{3,4} on areas larger than $1\ \text{cm}^2$.

At present, fundamental and technologically oriented research on nc-DSC run in parallel. While many academic research groups investigate the working principle aspects of the cell, several companies and research institutes have concentrated their efforts on the processing aspects, scaling up and stability aspects of the nc-DSC technology for indoor and outdoor applications.

In order to transfer results achieved with small laboratory cells to a full production line for dye-sensitized solar modules to be used for practical applications, all the process steps and technological parameters that are relevant to industrial production have to be investigated. Important topics that are essential for a reliable and cheap production technology that should lead to a successful market introduction are:

- large area deposition of uniform TiO_2 layers;
- development of methods for dye staining and electrolyte filling;
- internal electrical interconnection of individual cells;
- hermetic sealing of modules;
- long-term stability;
- evaluation of process steps in terms of costs;
- market demand.

The research on nc-DSC at ECN is primarily focused on the development and mechanization of production processes for large module area manufacturing. The first efforts in this direction were carried out in collaboration with a number of European research partners and were related to the production and testing of nc-DSC for indoor applications. Good reproducibility and indoor stability was achieved with multiple-layer screen-printing on large number of TCO-glass plates⁵⁻⁷ with sizes up to $10 \times 10\ \text{cm}^2$.

Since then, the mechanization of the individual process steps has continued and improved, which has resulted in the realization of a complete baseline at ECN for the production of nc-DSC. This baseline is presently used for the production of standard glass/glass devices on so-called $\text{SnO}_2\text{:F}$ masterplates with sizes up to $10 \times 10\ \text{cm}^2$. Depending on the application, different designs of cells and modules can be used, as will be described in this work.

In this paper, the different baseline processes are described for two types of nc-DSC of the standard glass/glass design. It is demonstrated that processing of larger numbers of nc-DSC in the baseline was successful in terms of reproducibility and yield.

2 DEVICE CONSTRUCTION AND BASELINE DESCRIPTION

2.1 Device construction

A schematic representation of the construction of the nc-DSC is presented in Figure 1. In the basic version, the device consists of two glass substrates on which a transparent conducting oxide (TCO i.e. $\text{SnO}_2\text{:F}$) with high optical transmission and low resistance is coated. On one side of the cell, the photoelectrode, a porous layer ($5\text{--}15\ \mu\text{m}$) of a wide-bandgap semiconductor is deposited composed of nanometer-sized particles ($10\text{--}20\text{nm}$) which are connected to form a three-dimensional conducting network. The material of choice is basically TiO_2 .

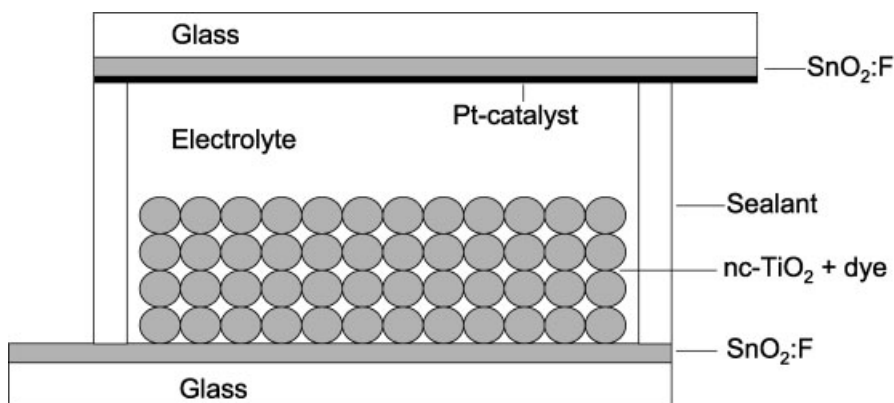


Figure 1. Schematic construction of a glass/glass nc-DSC

A monolayer of a sensitizing dye is adsorbed on the nanocrystalline oxide film. The second $\text{SnO}_2:\text{F}$ substrate is coated with a catalytic amount of platinum and serves as the counter-electrode. In a complete cell, photoelectrode and counter-electrode are clamped together and the space between the electrodes and the voids between the TiO_2 particles are filled with an electrolyte, containing a redox couple, usually iodide/triiodide (I^-/I_3^-) in a non-viscous organic solvent.

For the production and scaling up of practical solar cells on large areas, modules have to be constructed from individual cells. The relatively high sheet resistance of the $\text{SnO}_2:\text{F}$ coating (usually $\sim 10 \Omega/\text{square}$) used as the current collector, limits the width of the individual cells to less than 1 cm. One strategy to reduce ohmic resistance losses in a module is to interconnect many parallel single cells in series, which in practice means that the photovoltage of the modules increases while keeping the current relatively constant. Three types of series-connected nc-DSC module designs can be distinguished: a monolithic, Z- and W-type connection of individual cells and proof of concepts has been described in the literature.^{5,8-10} An alternative way to avoid ohmic losses is to apply a current collector grid to the conducting glass, quite similar to the silicon technology. In this design, high currents and low voltages are obtained. Since silver is usually the material of choice, it is of great importance to protect the silver grid adequately from the highly corrosive iodine-containing redox electrolyte, which is presently used in the dye solar cell.

Currently, two types of nc-DSC devices are manufactured as standard in the processing baseline.

1. A so-called master plate (Figure 2a) comprising five single cells on one $\text{SnO}_2:\text{F}$ glass substrate with an overall size of $10 \times 7.5 \text{ cm}^2$. $\text{SnO}_2:\text{F}$ glass is used for the photoelectrode and counter-electrode. This type of device is used in the baseline as the main research vehicle for testing new materials and components. Part of the processing of this type of master plate is briefly described elsewhere.¹¹ Two different designs have been applied in this investigation: the 'standard' masterplate consisting of five single cells with an active area of $4.0 (5.0 \times 0.8) \text{ cm}^2$. This design was primarily used for long-term stability tests¹¹ and not optimised for high efficiency. In particular, the distance (12 mm) between the current-collecting silver lines is too large, resulting in lower fill factors (up to 0.66), due to the series resistance losses in the TCO-layer. In order to overcome this, an improved design of the original concept was developed. The 'high-efficiency' master plate still consists of five cells with a reduced size of $2.5 (5.0 \times 0.5) \text{ cm}^2$ and 8 mm distance between the current collecting silver lines, resulting in higher fill factors (up to 0.71).
2. Single cells are manufactured on $\text{SnO}_2:\text{F}$ plates of $10 \times 10 \text{ cm}^2$ with an active area of 68 cm^2 , using a silver grid for current collection. A prototype of this device is shown in Figure 2b. The size of 100 cm^2 is chosen as representing a device with a realistic size for industrial processing. Moreover, for these type of devices only one electrolyte filling hole, drilled into the counter-electrode, is required, in contrast to series-connected modules where multiple holes are needed. In analogy to silicon solar cell wafer technology, a screen-printed grid of silver lines is deposited on the $\text{SnO}_2:\text{F}$ glass to reduce ohmic losses. The silver grid is protected against iodine-based electrolytes by using polymer-based hot-melt seal foil.

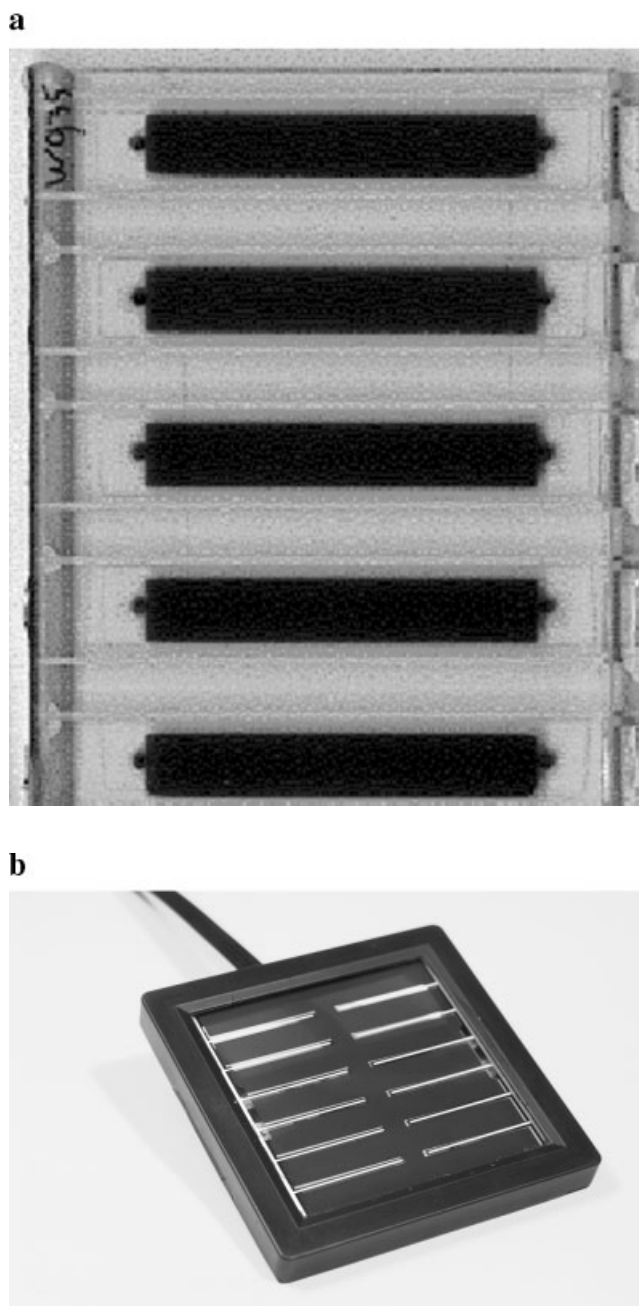


Figure 2. Photographs of a master plate containing five single cells: (a) type 1; (b) type 2, a framed current-collecting device of total area 100 cm^2 with an active area of 68 cm^2

2.2 Description of baseline process and equipment

In the following, the process steps used in the manufacturing of 'standard' glass/glass nc-DSC of types 1 and 2 are described.

1. Preparation of the glass
2. TiO_2 colloids and paste preparation
3. Screen-printing of active layers

4. Drying and firing
5. Sealing and foil attachment
6. Coloration
7. Lamination
8. Filling and hole closure
9. Wiring and framing

During the different process steps, accurate positioning of the SnO₂:F glass (electrode) is essential. To fulfill this requirement, outline units are used. These units make it possible to position the electrodes at three points with an accuracy of ± 0.1 mm with respect to the full length of the substrate (10 cm). The outline units are used for process steps 3, 5, 6 and 7.

2.2.1 Preparation of the glass

The SnO₂:F coated glass plates are precision pre-cut for mechanical alignment. Standard sizes are 7.5×10 cm² and 10×10 cm². In the concept of the masterplate, the single cells have to be electrically insulated. In order to realize this, insulation laser scribing of the SnO₂:F is applied. Hole drilling at the rear side electrode is required to obtain holes for electrolyte filling (step 8). After glass processing, the SnO₂:F substrates are stacked into cages and cleaned in an industrial washing machine using deionized water and detergents.

2.2.2 TiO₂ colloids and paste preparation

The TiO₂ colloids have been prepared by hydrolysis of titaniumisopropoxide in water (see experimental section for a detailed description). After peptization, a colloidal TiO₂ solution is obtained, containing TiO₂ particles with a size in the range of a few nanometers. To obtain TiO₂ particles of a desired size, a growth process is conducted in an autoclave, resulting in particle sizes between 20 and 40 nm, depending on conditions. The TiO₂ colloid is transferred from the aqueous solution into a terpeneol/ethylcellulose mixture to obtain a screen-printable paste, by means of a pearl mill.

2.2.3 Screen-printing of active layers

Screen-printing is used as the deposition technology in the baseline. In order to prevent contamination of dirt particles on the wet film, the printing step is carried out in a clean-room environment, using standard screen printing equipment (Ekra, DEK). The silver grid is printed onto photoelectrode and counter-electrode. Titanium dioxide as the photoconductive semiconductor on the front electrode and platinum as the catalyst on the counter-electrode are printed in single or multiple layers.

2.2.4 Drying and firing

A drying step for the screen-printed silver grid on the photoelectrode is necessary before the TiO₂ layer is deposited, otherwise the screen destroys the wet film during a follow-up print. This also holds for the silver grid on the counter-electrode before printing of platinum is realized. The printed TiO₂ layer has to undergo another drying step before firing in order to establish a well-controlled film structure and to prevent adherence of dirt particles to the wet film. For the drying step a belt furnace (Forced convection system) is used. The final firing step is carried out in two infrared sinter ovens (Gobi) where photo and counter-electrodes are fired at temperatures ranging from 450 to 500°C for 30 min. In total, 54 electrodes of size 10×10 cm² can be fired in one batch.

Process steps 1–4 are carried out with commercially available equipment. The further processing steps leading to sealed devices are carried out with dedicated equipment that has been developed from the laboratory stage.

2.2.5 Sealing and foil attachment (see Figure 3)

For the protection of the current-collecting grid a polymer hot-melt seal foil (Surlyn or Bynel) is applied. Bonding of the foil has to take place before staining, because during the coloration step dye molecules contaminate the SnO₂:F substrate. This hinders effective bonding of the foil onto the TCO. The foil is available as a gasket, consisting of Surlyn or Bynel and a protective polypropylene cover foil.



Figure 3. Pre-lamination unit for fixation of the polymer hot-melt to the TCO glass plates

After precise printing, accurate positioning of the seal foil is desirable. In order to do so, an alignment and tacking unit is in use, in which the (previously stamped-out) gaskets are positioned and locally attached to the glass.

The first step is to transfer the foil gasket onto the $\text{SnO}_2\text{:F}$ glass covering the current-collecting grid. The gasket is loaded into the mould of the alignment and tacking unit. Heatable rods, mounted to a carrier system, are transported through holes in the mould and press the gasket onto the surface of the glass substrate. The rods tack the gasket at 48 points accurately to the surface of the $\text{SnO}_2\text{:F}$ glass substrate. Completion of this process step is carried out by bonding the gasket firmly to the glass substrate with a vacuum assisted laminator.

2.2.6 Coloration (see Figure 4)

Two different methods of coloration in the device manufacturing can be distinguished. The first method is to stain the printed and fired TiO_2 glass substrate (photoelectrode) before sealing, as is carried out for the devices of type 2. In case of the masterplate design 1, a second method is used where photoelectrodes and counter-electrodes are fused together first and then stained by means of flushing the dye solution through an inlet and outlet port in the glass substrate.

Method 1 might be more viable if it comes to industrial production, because of fast staining of the full area. This can be done by chemical bath coloration, or full-area coloration in a staining chamber. A prototype machine is shown in Figure 4a. The working principle of a staining chamber is based on generating a turbulent flow of dye solution across the TiO_2 layer. Key parameters, which control the coloration process, are dye concentration, injection speed, pressure of the dye fluid, process temperature, thickness and porosity of the TiO_2 layer. After staining, the TiO_2 layer is flushed with pure solvent to remove unabsorbed dye molecules, and dried under nitrogen.

A closed circuit, consisting of a circulation pump and a staining chamber, is constructed through which the dye solution can be transported. The staining chamber is directly connected to a circulation pump. Concentrated dye solution is pumped from a reservoir and distributed to the staining chamber by a manifold. After staining, the dye solution is collected by another manifold and returned to the reservoir. A pattern of flushing holes located at the bottom of the chamber is designed to stain the electrode uniformly. Size and pattern of the holes make it possible to pressurize the dye solution and to create a turbulent flow.

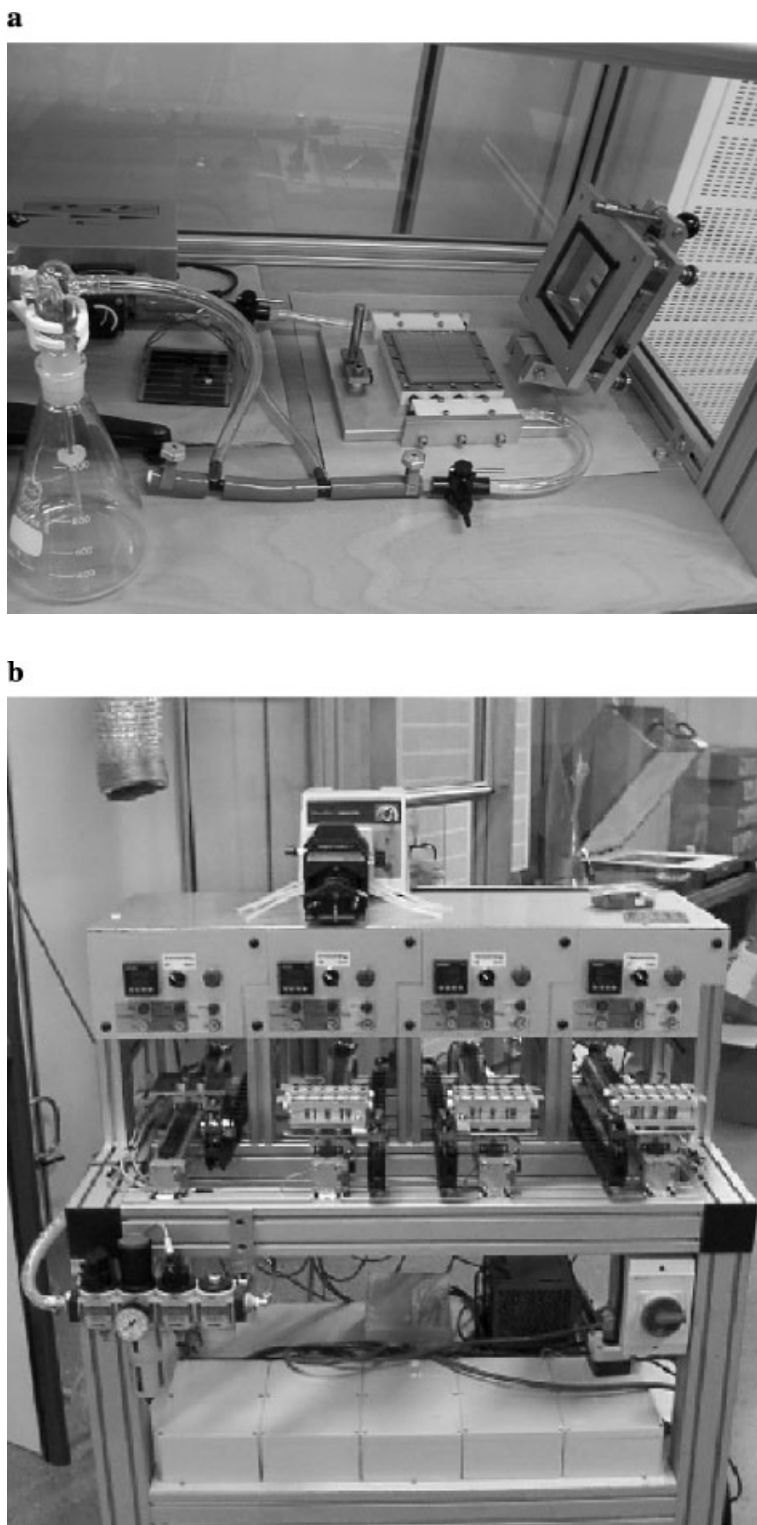


Figure 4. Staining chamber for full area coloration of the 100 cm² devices (a) and an automated pump-through coloration machine for master plate devices (b). This machine consists of four filling units, so that four master plate devices can be coloured simultaneously

The rim of the chamber is surrounded by a silicon-based sealing material to close the chamber hermetically towards the stained photoelectrode. Teflon is used as a basic material for all components in order to be inert to the dye solution. Staining can be optically controlled through a glass plate cover. To increase the speed of the coloration the dye solution is heated.

The second method 'first seal then stain' is mainly used if both photoelectrode and counter-electrode are fused together by using other sealing materials that require higher operating temperatures (e.g., glass soldering). Glass soldering is carried out at high temperatures ($>600^{\circ}\text{C}$), where the dye decomposes. In this case coloration takes place after fusing by pumping the dye through an inlet port into the cell and draining it through an outlet port (see Figure 4b). The electrodes can be moderately heated during the staining process in order to increase the rate of adsorption of dye molecules. This technique is used for controlled coloration of cells with smaller surface areas.

2.2.7 Lamination of photo- and counter electrode (see Figure 5)

A new concept of lamination has been developed that enables heating of both electrodes during lamination. To reduce the sealing time a pneumatic press assists the sealing step. The complete sealing process is carried out under vacuum, in order to prevent air inclusions in the molten seal foil. A main feature of the vacuum-assisted laminator is that process parameters such as temperature, vacuum level, sealing time and seal pressure can be adjusted, measured and actively controlled. The vacuum laminator is designed as a semi-automated machine, which means that the electrodes to be sealed are manually loaded and unloaded. From this point onward all sealing steps are controlled by PLC.

The vacuum assisted laminator is able to handle the bonding of the seal foil gasket onto the $\text{SnO}_2:\text{F}$ glass substrate and also the final step of assembling photoelectrode and counter-electrode together. Before assembling the photoelectrode and counter-electrode, the protective polypropylene cover foil has to be removed from the photoelectrode and counter-electrode.

2.2.8 Rear-side filling and hole closure

In the case of the masterplates of type 1, a pipette tool is used to fill the holes with the electrolyte solution.



Figure 5. Vacuum laminator press for lamination of photoelectrode and glass counter-electrode with a polymer hot-melt

For devices of type 2, a method for mechanical one-hole electrolyte filing has been developed. Innovative equipment for vacuum-assisted filling is in operation. After filling, the hole is closed with polymer hot-melt foil and a thin cover glass, using a hot-press sealing stamp.

2.2.9 Wiring and framing of devices 1 and 2

The last step is wiring and framing. The wires are soldered on to the terminals, and the entire device can be mounted into a polyurethane frame for further protection of the electrical contacts, as is done for the type 2 devices.

3 EXPERIMENTAL DETAILS

3.1 Materials

The basic material of the electrodes is SnO₂:F coated glass (LOF-TEC8, 3 mm, 8 Ω/square). The sensitizing dye used is *cis*-di(thiocyanato)-*N,N'*-bis(2,2''bipyridyl-4,4'-dicarboxylate)Ru(II)bis-tetrabutylammonium (known as N719, supplied by Solaronix) as a 0.5 mM solution in a 50/50 (vol/vol) mixture of acetonitrile and *tert*-butanol.

Devices have been filled with electrolyte of the following composition: 0.1 M LiI, 0.05 M I₂, 0.5 M *tert*-butylpyridine (TBP) and 0.6 M hexylmethylimidazolium Iodide (HMII) in acetonitrile solvent. Surlyn 1702 and Bynel polymer hot-melt foil have been used as primary sealing materials.

The platinum screen-printable paste was based on H₂PtCl₆ dispersed in a mixture of terpineol and ethylcellulose. The silver paste used is Ferro SP 1248 conductive paste.

3.2 Preparation of the TiO₂ colloids

The colloids have been prepared according to procedures reported earlier.^{12,13} A typical synthesis of TiO₂ colloid is carried out as follows: 383 g titanium tetraisopropoxide was rapidly added to 750 ml distilled water and stirred for 1 h. A white precipitate was formed instantaneously by hydrolysis of the titanium isopropoxide, which was filtered using a glass filter and washed three times with small portions of distilled water. The filter cake was then transferred into a titanium autoclave and mixed with 29.3 g of 25% tetraethylammonium hydroxide (TMAH) solution. Peptization occurred during heating the mixture in the autoclave at 130°C for approximately 12 h. To realize particle growth up to the desired size of approximately 20 nm the resulting suspension was treated to 12 h hydrothermally in an autoclave at temperatures ranging from 150 to 280°C.

The colloidal particles were transferred from the aqueous suspension into a mixture of terpineol and ethylcellulose to prepare a screen-printable paste.

3.3 I–V characterization

I–V characteristics of the devices (I_{sc} , V_{oc} , FF and η) are derived with a Keithley 2400 source meter. The devices under test are illuminated under a metal halide lamp with 1 sun equivalent (Steuernagel solar constant 575 solar simulator, 1000 W/m² at room temperature). The Steuernagel solar simulator is set to AM1.5 conditions after calibration of a nc-DSC using a calibrated reference silicon solar cell. Spectral mismatch was taken into account using methods described elsewhere.^{14,15}

Relaxation time of the devices after processing and before measuring is set to 1 h.

4 RESULTS AND DISCUSSION

4.1 Upscaling of cell surface area

As mentioned in Section 2, two types of devices are processed in the baseline:

1. the 'masterplate': total area 75 cm², active area per cell 4 or 2.5 cm²;
2. the 'current-collecting device': total area 100 cm², active area 68 cm².

Typical I - V data obtained from standard cells on the master plate of type 1 are short-circuit current densities (J_{sc}) up to 13 mA/cm^2 , open-circuit voltages (V_{oc}) of 0.7 V and fill factor (FF) of 62 – 71% (depending on the type of master plate) under optimal conditions resulting in efficiencies (η) up to 6% . Enlarging the device area from laboratory size (2.5 or 4 cm^2 active area) to an active surface area of 68 cm^2 generates a lot of knowledge relevant to manufacturing under realistic industrial process conditions. In the first place, cell efficiencies achieved on master plates have been reproduced on devices of type 2 using the same cell ingredients. A cell efficiency of 5.9% was reached for an active area of 68 cm^2 , equal to the above-mentioned efficiency of 6% for 2.5 cm^2 cells on a masterplate under equal processing conditions.

This result proves that scaling up of the cell surface area is possible, generating the same cell efficiencies as for small cells with areas $<5 \text{ cm}^2$. The scaling up also revealed new critical processing steps. For example the firing of large glass plates proved to be a critical step and requires a more controlled heating process than for small devices. Minute warping of the glass during the firing process can be detrimental, as it is essential to have flat parallel plates in order to be able to seal the devices. This problem has been solved by cooling more slowly after the firing process.

Scaling up the total device up to $10 \times 10 \text{ cm}^2$ or even larger also leads to problems with efficient current collection. In the case of current-collecting devices more active cell area with respect to total area has to be sacrificed to minimize ohmic losses. This problem should be considered in scaling up, since the silver grid has to be protected by sealing material that occupies a relatively large surface. This results in a decrease of the ratio (active area/total area) with increasing size of the devices, unless special measures are taken to overcome this. In the 100 cm^2 devices of type 2 which are presently constructed in the baseline this ratio is 0.68 , which means that the cell efficiency drops to around 4% with respect to total area. It should be noted that the present design is chosen in the first place for ease of fabrication and handling of the devices. The future challenge is to find solutions for the optimisation of the ratio (active area/total area) thereby maintaining the current density and minimizing resistance losses. On the other hand, non-active areas can also be used to improve the light management of the cell, for instance by applying scattering sealants or white reflecting spaces.

4.2 Reproducibility of the baseline

The reproducibility of the baseline process was tested by processing 27 devices of type 2 in one run on a single day. This experiment was focused on reproducibility and not on optimization of the cell efficiency. The distribution of J_{sc} , V_{oc} , FF and η for the 27 devices is shown in Figure 6. One device of the 27 was out of range due to human errors as is clearly visible in the histograms. This results in an overall yield of the baseline process of 96% . In Table I, the average values of the I - V parameters together with the deviations for the remaining 26 cells are presented. As can be seen from the table, the deviations in the single I - V parameters J_{sc} , V_{oc} and FF are fairly low for the majority of devices: all deviations are $<4\%$ for at least 23 devices (88% of total). The deviations add up in the efficiency values as is indicated by somewhat larger deviations in η . The majority of the group of 26 devices (22 devices, 84% of total) show a maximum deviation of 7% from the average η value of 4.3% (based on the active surface area of 68 cm^2). From this it can be concluded that the reproducibility of the baseline process is excellent.

4.3 Reproducibility of TiO_2 colloid synthesis

The reproducibility of the processing of 100 cm^2 devices on the baseline is proven in the previous section. The preparation of TiO_2 was not included in this test as one batch of TiO_2 was used for the total number of 27 devices. In a parallel test, the reproducibility of TiO_2 preparation was studied by comparing three different TiO_2 batches, all prepared in a similar way.

In Table II, the BET surfaces and primary particle size (by X-ray analysis) are presented for the three batches of colloid. The deviations in BET and primary particle size are small, indicating a reproducible colloid synthesis. This is further supported by the results of cell performance tests on these three batches of colloid.

Using master plates of type 1 (2.5 cm^2) as the test device the reproducibility of the complete processing of nc-DSC including the TiO_2 synthesis is illustrated in Figure 7, showing η , J_{sc} , V_{oc} and FF from three batches of

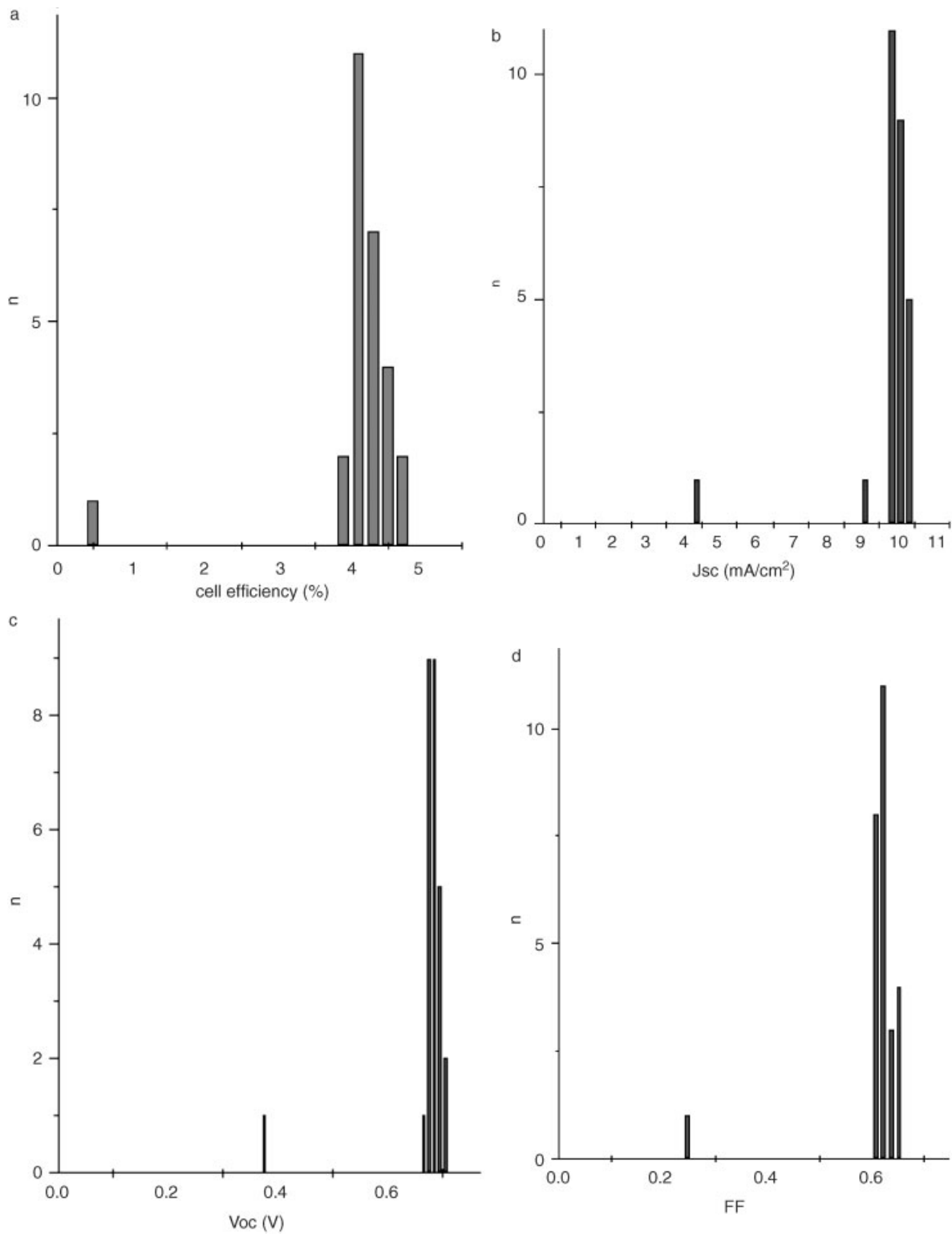


Figure 6. Distribution of I - V parameters: (a) efficiency η (%); (b) J_{sc} (mA/cm²); (c) V_{oc} ; (d) fill factor FF for 27 10×10 cm² devices (active area 68 cm²)

Table I. Average I - V parameters for 26 cells (total area 100 cm^2 , active area 68 cm^2) and deviations from average

J_{sc} (mA/cm ²)	V_{oc} (V)	FF	η (% active area)
10	0.68	0.62	4.3
Deviations (%)			
1 cell: 9	1 cell: 3.4	1 cell: 5.5	3 cells: 9–10
1 cell: 4.6	2 cells: <2.7	1 cell: 4.9	1 cell: 7.7
24 cells: <3.4	23 cells: <2	24 cells: <4.1	22 cells: <7

Table II. BET surface and primary particle size for three batches of TiO₂, prepared by similar procedures (see experimental section)

Batch	BET (m ² /g)	Primary particle size (nm)
A	38	35
B	36	30–35
C	38	35

alkaline colloid prepared according to equivalent procedures. For each batch, one master plate containing five individual nc-DSC was prepared. One cell (batch A, last cell) shows a very poor FF, probably due to a contacting problem, and is not considered further. The maximum deviation from the average I - V parameters η , J_{sc} , V_{oc} and FF on one master plate is 5%. The deviation in the average values for the cell efficiencies between the three batches of colloid (three master plates) is at most 3.2%. These results prove that the complete manufacturing process of nc-DSC, starting with the colloid synthesis, at ECN is reproducible with a cell efficiency of 4.9% for this specific type of colloid under standard test conditions (AM G1.5, 1000 W/m^2 , 25°C). As mentioned before, higher efficiencies up to 6% have been achieved with master plates.

5 CONCLUDING REMARKS

A complete semi-automated baseline for reproducible manufacturing of nc-DSC on sizes up to $10 \times 10\text{ cm}^2$ is described. The baseline consists partly of dedicated equipment that has been designed and developed from the laboratory stage. No automation is introduced between the individual processing steps.

Two types of glass/glass devices with different designs are presently constructed in the baseline, i.e., with active areas of $<5\text{ cm}^2$ and 68 cm^2 . By using the same cell ingredients and components, it has been shown that AM1.5 power conversion efficiencies around 6.0%, obtained for small cells ($<5\text{ cm}^2$), can successfully be translated to 100 cm^2 devices for which a maximum power conversion of 5.9% based on active area (68 cm^2) is achieved.

Scaling up of this technology from laboratory size to larger areas generally leads to a loss of active area with respect to total area, resulting in lower current densities. For the devices described in this work, the ratio (active area/total area) is 68/100, resulting in a power conversion efficiency of 4% with respect to the total area of the device.

Processing of a single day's production of $27\ 10 \times 10\text{ cm}^2$ nc-DSC has been successful in terms of yield and reproducibility. The yield was 96% (26 of 27 devices) while 84% (22 of the remaining 26 devices) generated a cell efficiency within 7% deviation from the average value. It has also been demonstrated that reproducible devices can be constructed in the baseline when different batches of identically prepared TiO₂ colloids are used.

In order to achieve commercialization of this technology for low-power and high-power applications, more fundamental and technological research is required to answer key questions related to efficiency, long-term stability, manufacturability and scale-up of production.

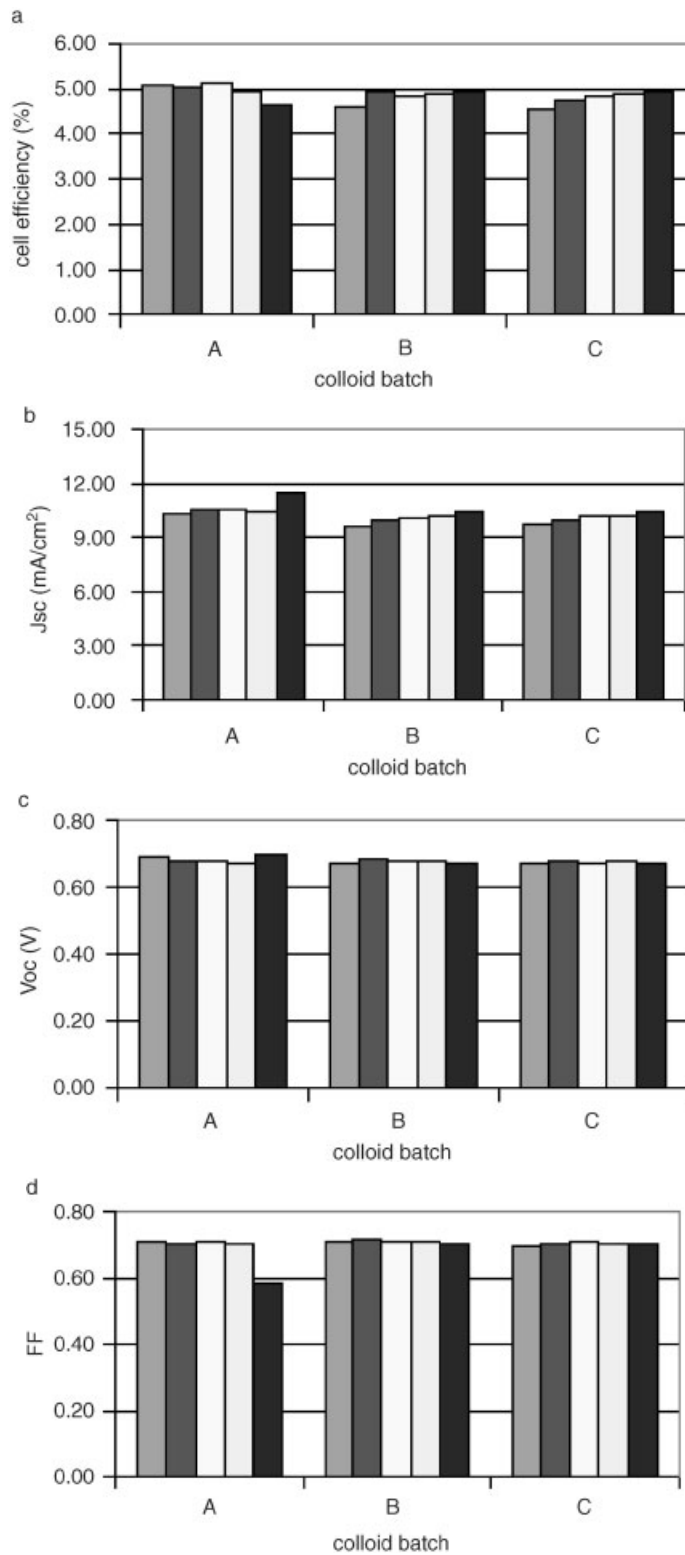


Figure 7. I - V parameters: (a) efficiency η (%); (b) J_{sc} (mA/cm²); (c) V_{oc} ; (d) fill factor FF for three different TiO₂ colloid batches prepared by similar procedures

With the presently described baseline and standardized approach, and promising results on reproducibility and yield, a firm basis has been established to carry out reliable and meaningful studies in this field and to find out how the above-mentioned issues can be combined to achieve the low cost potential of this technology.

Acknowledgments

We thank: Dr T. Meyer and A. Meyer (Solaronix SA, Switzerland), Dr J. Wilkie and I. Gregory (Shell Solar, Netherlands) for valuable discussions and collaboration; Dr A. Hinsch (FhG-ISE, Germany) for his contribution to the development of parts of the baseline during his work-period at ECN. This work was partly carried out with financial support from the Netherlands Organization for Energy and the Environment (Novem) (Contract 146-120-021-1) and the ECN-ENGINE program.

REFERENCES

1. O'Regan B, Grätzel M. A low cost, high-efficiency solar cell based on dye-sensitized colloidal TiO₂ films. *Nature* 1991; **353**: 737–739.
2. Green MA, Emery K, Bücher K, King DL, Igari S. Solar cell efficiency tables (version 11). *Progress in Photovoltaics: Research and Applications* 1998; **6**: 35–42.
3. Hinsch A, Kroon JM, Kern R, Sastrawan R, Meyer A, Uhlendorf I. Long-term stability and efficiency of dye-sensitized solar cells. *Proceedings of the 17th European Photovoltaic Solar Conference and Exhibition*, Munich, 2001; 51–54.
4. Green MA, Emery K, King DL, Igari S, Warta W. Solar cell efficiency tables (version 20). *Progress in Photovoltaics: Research and Applications* 2002; **10**: 355–360.
5. Burnside S, Winkel S, Brooks K, Shklover V, Grätzel M, Hinsch A, Kinderman R, Bradbury C, Hagfeldt A, Pettersson H. Deposition and characterization of screen-printed porous multi-layer thick film structures from semiconducting and conducting nanomaterials for use in photovoltaic devices. *Journal of Materials Science: Materials in Electronics* 2000; **11**: 355–362.
6. Hinsch A, Kinderman R, Wolf M, Bradbury C, Hagfeldt A, Winkel S, Burnside S, Grätzel M, Pettersson H, Johander P. Dye sensitized solar cells; large scale batch processing of mini modules for application in consumer electronics. *Technical Digest 11th International Photovoltaic Science and Engineering Conference (PVSEC-11)*, Sapporo, 1999; 869–870.
7. Pettersson H, Gruszecki T. Long-term stability of low-power dye-sensitised solar cells prepared by industrial methods. *Solar Energy Materials and Solar Cells* 2001; **70**(2): 203–212.
8. Kay A, Grätzel M. Low cost photovoltaic modules based on dye sensitized nanocrystalline titanium dioxide and carbon powder. *Solar Energy Materials and Solar Cells* 1996; **44**: 99–117.
9. Chmiel G, Gehring J, Uhlendorf I, Jestel D. Dye sensitized solar cells (DSC): progress towards application. *Proceedings of the 2nd World Conference and Exhibition on Photovoltaic Solar Energy Conversion*, Vienna, 1998; 53–57.
10. Grätzel M. Perspectives for dye-sensitized nanocrystalline solar cells. *Progress in Photovoltaics: Research and Applications* 2000; **8**: 171–185.
11. Hinsch A, Kroon JM, Kern R, Uhlendorf I, Holzbock J, Meyer A, Ferber J. Long-term stability of dye-sensitised solar cells. *Progress in Photovoltaics: Research and Applications* 2001; **9**(6): 425–438.
12. Barbé CJ, Arendse F, Comte P, Jirousek M, Lenzmann F, Shklover V, Grätzel M. Nanocrystalline titanium oxide electrodes for photovoltaic applications. *Journal of the American Ceramic Society* 1997; **80**(12): 3157–3171.
13. Burnside SD, Shklover V, Barbé C, Comte P, Arendse F, Brooks K, Grätzel M. Self-organization of TiO₂ nanoparticles in thin films. *Chemistry of Materials* 1998; **10**(9): 2419–2425.
14. Sommeling PM, Rieffe HC, Roosmalen JAMV, Schönecker A, Kroon JM, Wienke JA, Hinsch A. Spectral response and IV-characterization of dye-sensitized nanocrystalline TiO₂ solar cells. *Solar Energy Materials and Solar Cells* 2000; **62**: 399–410.
15. Kroon JM, Wienk MM, Verhees WJH, Hummelten JC. Accurate efficiency determination and stability studies of conjugated polymer/fullerene solar cells. *Thin Solid Films* 2002; **403–404**: 223–228.